



HAL
open science

MOSAIC GLAO performance and system architecture: AO for the entire ELT focal plane

Nazim A Bharmal, Timothy J Morris, Timothy Butterley, Polly Gill, Jurgen Schmoll, Noah Schwartz, David G Bramall, Christopher Davison, Jay Stephan, Raziye Artan, et al.

► **To cite this version:**

Nazim A Bharmal, Timothy J Morris, Timothy Butterley, Polly Gill, Jurgen Schmoll, et al.. MOSAIC GLAO performance and system architecture: AO for the entire ELT focal plane. Adaptive Optics Systems IX, Jun 2024, Yokohama, Japan. pp.132, <10.1117/12.3019113>. <hal-04976615>

HAL Id: hal-04976615

<https://hal.science/hal-04976615v1>

Submitted on 6 Mar 2025

HAL is a multi-disciplinary open access archive for the deposit and dissemination of scientific research documents, whether they are published or not. The documents may come from teaching and research institutions in France or abroad, or from public or private research centers.

L'archive ouverte pluridisciplinaire HAL, est destinée au dépôt et à la diffusion de documents scientifiques de niveau recherche, publiés ou non, émanant des établissements d'enseignement et de recherche français ou étrangers, des laboratoires publics ou privés.



Distributed under a Creative Commons CC BY 4.0 - Attribution - International License

MOSAIC GLAO performance & system architecture: AO for the entire ELT focal plane

Nazim Ali Bharmal^a, Timothy J Morris^a, Timothy Butterley^a, Polly Gill^a, Jürgen Schmall^a, Noah Schwartz^b, David Bramall^a, Christopher Davison^a, Jay Stephan^b, Raziye Artan^b, Phil Parr-Burmann^b, R. Pello^c, M. Puech^d, É. Prieto^c, M. Rodrigues^d, R. Sanchez-Janssen^b, G.B. Dalton^{e,f}, F. Ducret^c, K. El Hadi^c, M. L. García-Vargas^{g,h}, and J. Lynnⁱ

^aCentre for Advanced Instrumentation, Durham University, South Road, Durham DH1 3LE, United Kingdom

^bUKRI-STFC UK Astronomy Technology Centre, Blackford Hill, Edinburgh EH9 3HJ, United Kingdom

^cAix Marseille Université, CNRS, CNES, LAM (Laboratoire d'Astrophysique de Marseille), UMR 7326, 13388 Marseille, France

^dGEPI, Observatoire de Paris, PSL University, CNRS, 92190 Meudon, France

^eDept. Physics, University of Oxford, Keble Road, Oxford, OX1 3RH, UK

^fRAL Space, Science and Technology Facilities Council, Harwell, Didcot, OX11 0QX, UK

^gFRAGMENT SLNE, Calle Tulipán 2, portal 13, 1A, E-28231 Las Rozas de Madrid, Spain

^hDpto de Física de la Tierra y Astrofísica, Fac. CC Físicas, Universidad Complutense de Madrid, Plaza de las Ciencias, 1, E-28040 Madrid, Spain

ⁱNOVA Optical IR Instrumentation Group, ASTRON, Netherlands

ABSTRACT

MOSAIC is a wide-field spectrograph, combining multiple-object spectroscopy and integral field units, to cover the ELT focal plane with a field-of-view of 7.8 arcmin from the blue to the near-infrared, 390–1800nm. In the current Phase B design, AO is GLAO supported by four LGS in a fixed asterism and with multiple NGS. Although the GLAO correction is modest compared to other ELT instrumentation, the use of the integrated M4/M5 correction elements and the existing LGS allows for an efficient design which is outlined. MOSAIC GLAO will use the ELT PFS guide-probes to compensate for high-frequency tip/tilt errors, greatly relaxing the requirements on the instrumental NGS sensors. The Phase A architecture used the same pick-off mirrors as the IFU instruments to feed the NGS-WFS from anywhere in the focal plane, which was mandatory for the proposed MOAO design. The reduced performance requirements at Phase B allows us to take advantage, instead, of the four 2 arcmin diameter field-of-view through the LGS cutouts, arranged in a square pattern at an off-axis distance of 3.75 arcmin. In each LGS cutout, a wide-field-imager is implemented—alongside one LGS WFS—to acquire multiple NGS that supports both slow tip/tilt measurements, isolating instrument-Nasmyth flexure, solving for the astrometric distortion expected from errors in the ELT optical path, and supporting the alignment of MOS apertures with the field. The latter is a key requirement for MOSAIC, leading to 40mas accuracy in MOS aperture positioning and 40mas rotation displacement at the edge of the scientific field.

Keywords: ELT, MOSAIC, GLAO, LGS, Phase B

1. INTRODUCTION

MOSAIC is the ELT MOS-IFU instrument using 270 focal plane pick-offs over a field-of-view of 7.8 arcminutes, from blue through NIR (390–1800nm) with moderate spectral resolution. For a more complete description, please

Further author information: (Send correspondence to N.A.B.)

N.A.B.: E-mail: n.a.bharmal@durham.ac.uk

see paper 13096-41 from this meeting.¹ The key architecture that enables accessing over 75% of the curved ELT focal plane is the arrangement of tiles each containing a positioner which can either focus light into fibres for visible or NIR spectrographs, or direct light towards other optics that focus light into separate fibres for 8 NIR IFUs. The LGS light passes through four off-axis apertures, as shown in figure 1, and NGS are also observed through these apertures: this design choice restricts our technical field-of-view for NGS but improves stability and per-sensor field-of-view.

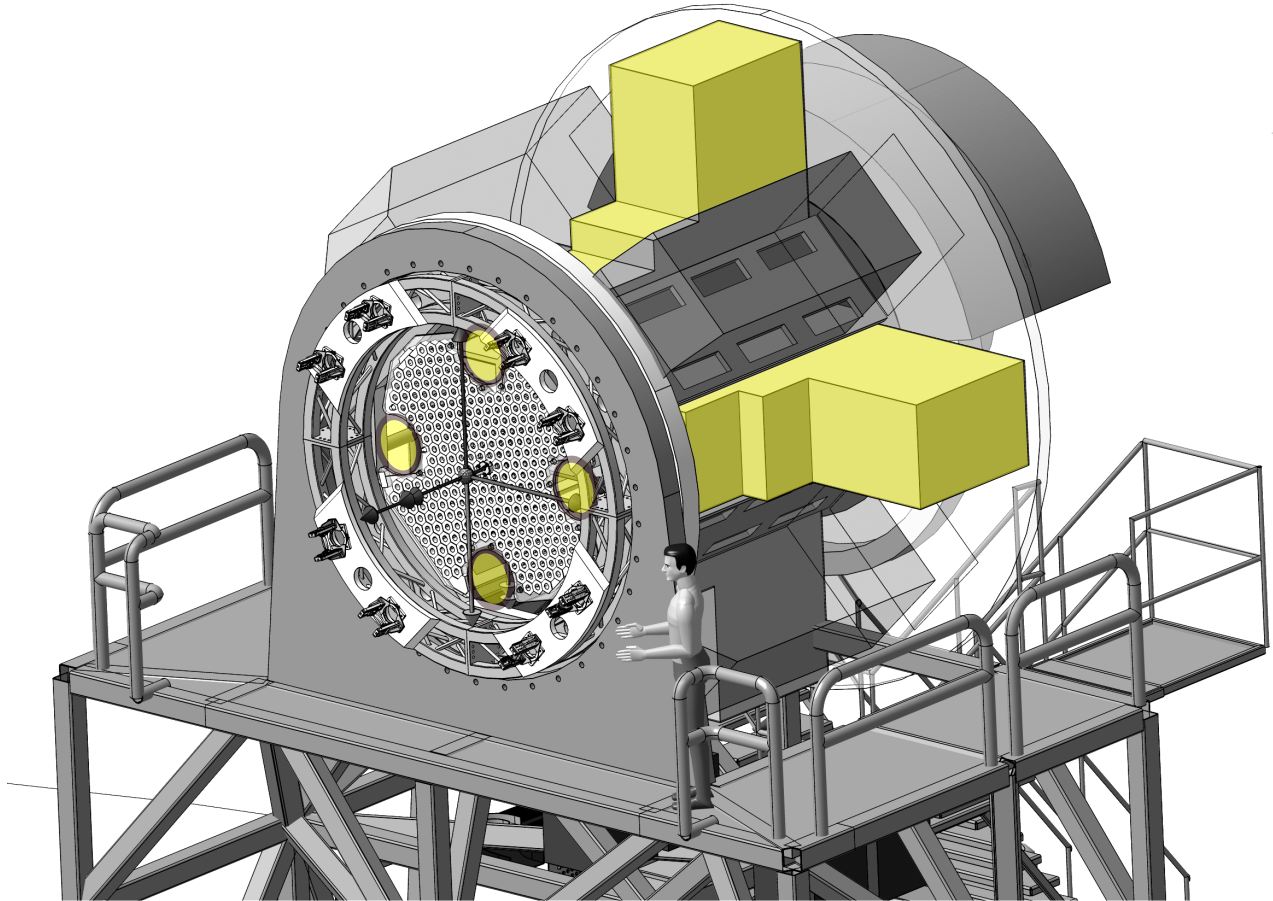


Figure 1. The MOSAIC instrument as envisaged on the Nasmyth platform. In this view we only show those components relevant to GLAO in yellow: the four LGS apertures or cutouts in the focal plane and two of the four associated GLAO Boxes (GBOXs) which contain, in turn, one NGS sensor and one LGS sensor each. Not shown is the other GLAO infrastructure which includes cabling and also the RTC (AOCM) which is located in the ELT Computer Room, as well as the LGS projectors (on the telescope), the adaptive M4/M5 (on the telescope), the Pre-Focal Station and associated Guide-Probes (directly in front of MOSAIC), and the Central Control System (in the ELT Computer Room). (courtesy, Laurent Martin, LAM.)

The GLAO sub-system of MOSAIC delivers adaptive optics correction sufficient to meet the specifications: in short, to prevent flux losses due to object–aperture misalignment and to increase flux coupling into the aperture. The first is achieved by accurate and precise estimation of the ELT astrometric solution, to account for focal plane distortions that move objects from their expected positions, and to ensure that MOSAIC remains aligned in terms of sky position (X-Y) and position angle (rotation) to the ELT. The second is from applying AO using on-instrument WFSs and, via the MOSAIC RTC (AOCM) and ELT Central Control System² (CCS), controlling the M4/M5^{3,4} deformable mirrors. In addition, the vibrations and misalignments caused by the large physical structures together with the additional measurements available from the ELT Pre-Focal Station⁵ (PFS) are also considered in our design. The reason for the design choice of GLAO is straightforward: the apertures we consider

are coarse, 150–600 mas, and the requirement for enclosed energy is an increase by $1.2\text{--}1.5 \times$ (for a $ZA=45^\circ$ and median atmospheric conditions). In simulation we see that the largest increase is for the worst seeing, by upto $\sim 70\%$. All together, we can state that the aim is to prevent MOS (600 mas apertures) aperture coupling variation with seeing and ELT–MOSAIC misalignments to less than 2%, and for the smaller IFU apertures (150 mas) a loss of less than 5% is the goal.

Unlike other ELT science instruments—for example, HARMONI, METIS, or MICADO to name three that have spatial resolution specifications—MOSAIC has no spatial resolution requirements and our spaxel scales are coarse (at least a factor of $10\times$ beyond the diffraction limit). Therefore Strehl ratio is a misleading performance metric and instead Enclosed Energy (EE) is what will be used in this work. In passing we note that in Phase A,⁶ MOSAIC did implement MOAO and but also in this case EE was the requirement. The increase in IFU spaxel size by a factor of two leads to the same conclusion of GLAO delivering appropriate EE when considering, for example, the science goal of galactic kinematics.

MOSAIC has a ADC in each pick-off arm—a positioner* which contains optics to relay the focus through the ADC and reimages the focus onto one of two fibre bundles for either visible low-resolution, visible high-resolution, or near-IR spectrographs. There is no plan for the GLAO sensors to incorporate a ADC therefore there is a potential offset between GLAO-derived object position and the positioner reimaged location. Therefore one calibration stage is understanding the performance of positioners and the dispersion of NGS targets in order to remove spectral-gradient offsets.

Furthermore, the ELT deploys upto 3 Guide-Probes⁷ from the PFS which are moderate-order NGS WFSs that operate at ~ 500 Hz. These wavefront sensors are *not* located on the instrument but nonetheless use the field from 2.5’-to-5’ radius. Necessarily, therefore, it is appropriate to ask the ELT to operate in ‘Cascade’ mode where the telescope operates its mirrors for tip/tilt correction from 40 Hz to the loop-rate limit. The remaining signals, upto 40 Hz, are the responsibility of the instrument. These are provided by the NGSS module. Thus control of tip/tilt is joint ELT/MOSAIC: the high-frequency signals, principally the atmosphere, are measured by the ELT and handled internally, and the low-frequency signals coming from the atmospheric residuals, telescope vibrations, and MOSAIC–Nasmyth platform movement (which can be significant) are resolved by the NGSS, processed by the AOCM, and then sent to the ELT CCS to be integrated with the high-frequency PFS measurements.

Finally, four laser guide stars are projected⁸ from the ELT to an asterism with radius 3.75’ and positioned equidistance: effectively the corners of a square. These follow the sky so the field-of-view to a radius of 1’ around each LGS are lost to permit the LGS through apertures in the MOSAIC focal plane, and then to four LGSS modules which each contain one LGS WFS. These Shack-Hartmann WFS are not yet fully specified but we expect similar parameters to those used in other ELT instruments and a preliminary set of design parameters will be discussed.

The telemetry data from the LGSS and NGSS together with the PFS tip/tilt signals sent to the MOSAIC RTC are all stored in a short-term engineering archive, which is available for post-observation processing to produce a variety of parameter estimations. These would include low-level analyses such as AO parameters (seeing, Fried parameter, C_n^2 profile) or at a higher level for PSF estimation. Currently this latter topic is under discussion with the science team so we note that the ELT infrastructure includes a fast AO model⁹ and we intend to use this to characterise the observation’s PSFs as a baseline proposal.

2. GLAO ARCHITECTURE AND INITIAL DESIGN

It is important to note that the GLAO sub-system places a strong constraint on sky coverage: the instrument requirement is $\gtrsim 99\%$ and cosmological fields are of interest. Accordingly using first estimates of the NGSS performance required as a minimum to resolve X-Y and rotation errors, alongside with plate-scale and an anamorphic mode which retains areal intensity (equal but opposite contractions in orthogonal axes) suggests that 1s exposures provide sufficient signal over 10,000 random all-sky pointings and accounting for the allocation

*Paper 13096-214, M. Thurneyson et al., this meeting

of 3 guide-stars to the PFS with a 75% probability that no LGS aperture is obscured[†] by a PFS guide-probe arm, to cover more than 99.5% of the sky. An example of a MOSAIC sky pointing configuration (*not* optimized for GLAO) is shown in figure 2: a rotation of the LGS asterism to permit 5 guide-stars to enter the NGSS field-of-view, as explained next, would be the next stage, but this image demonstrates how the focal plane is arranged.

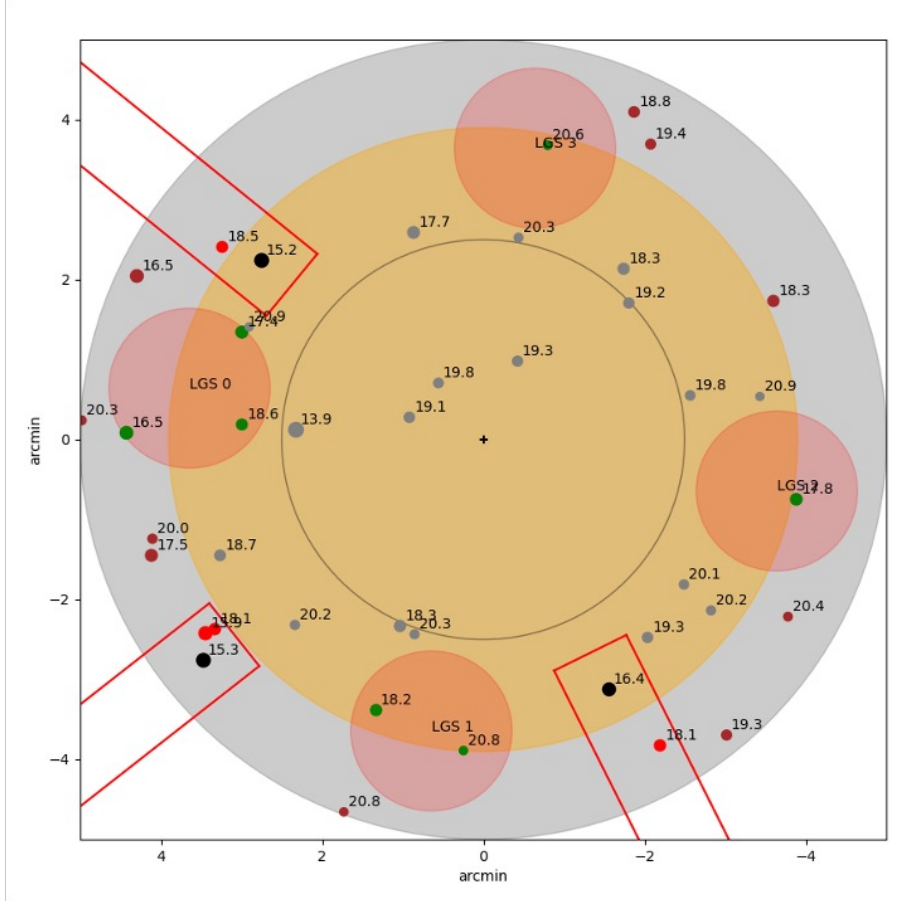


Figure 2. The MOSAIC field-of-view from the perspective of GLAO. The inner, yellow region is the scientific field-of-view—3.9' radius—with a boundary at 2.5' radius within which no vignetting by the PFS can occur. The outer circle, grey, is the entire ELT field-of-view with 5' radius. At 3.75' off-axis, every 90 degrees, is a LGS cutout within which the science field is not accessible since these are apertures which permit LGS beams to pass through to the GLAO Boxes containing the LGSS and NGSS sensors. The red boxes mark a nominal vignetting by three PFS arms (in this configuration) and we have allocated the three brightest stars according to the PFS requirements. (At this time, we do not choose to balance PFS coverage with minimising science vignetting: the upper left and bottom right arms both intrude into regions covered by positioners and so deny targets located there). Finally, within each LGS cutout, the stars available to the PFS (based on GAIA DR2 measurements) are shown in green. Due to our design, we can use 5 of the seven stars shown for the NGSS (guiding and slow tip/tilt), with at least one in each LGS cutout. (courtesy, Jay Stephan.)

We now discuss how light passes through one LGS cutout and is interfaced to the two sensing modules contained within the associated GBOX: the Laser Guide-Star Sensor and the Natural Guide-Star Sensor, LGSS and NGSS respectively. A sketch of a GBOX is shown in figure 3 and there are three modules: the Core

[†]For the remaining 25% of pointings where there is an obscuration, we have not yet fully studied modifying the vignetting nor the effect of ignoring that LGS although there are indications for both approaches that our needs are still met.

Structure, the LGSS and the NGSS. The Core Structure provides an interface to each AO sensor and in addition acts differently on the NGS and the LGS light. For NGS the beams are collimated by the core structure lens of 400 mm diameter which is used for both the NGS and LGS trains and called L1 in the following. For the NGS, this lens collimates the beams so that it forms a focal reductor with the following fast camera optics, imaging the 1.6 arcmin field onto a 20 mm detector. A dichroic plate behind L1 reflects the LGS beam of 589 nm wavelength, and as this beam is conjugated to the mesospheric sodium layer, L1 acts like a Shapley lens, increasing the system speed. This allows to reduce the migration of the focal point caused by the changing zenith distance from several meters to about 100 mm, which then can be collimated by an LGS collimator to feed the Shack-Hartmann sensor. At the time of the writing, the detailed design of the LGS optics is still pending.

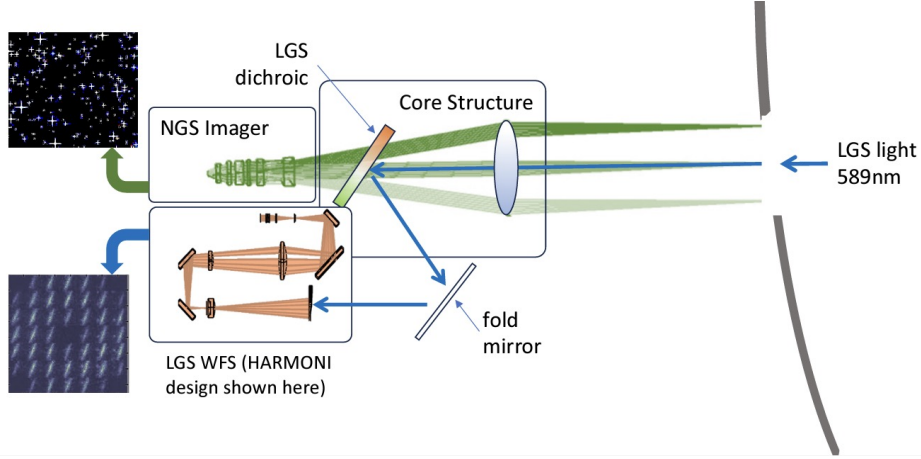


Figure 3. A sketch of a GBOX. On the right is the curved ELT focal plane and associated beams of light (LGS and NGS) which are tilted due to the lack of telecentricity. In green/orange are shown light from the LGS (also the arrows show the same light path) and in green is the light from the NGS. A shared module, the Core Structure, increases the beam speed/collimates LGS/NGS light, and then a dichroic sends 589 nm light to the LGSS. The through-beam is for the NGSS which is an imager, operating at 850–950 nm, over a 1.6' field-of-view with 0.1 arcsec pixel sampling.

The NGSS is actually conceived of an imager over (at least) 1.6' field-of-view, in order to match the technical detector (ESO LISA¹⁰) and is designed to operate between 850–950 nm. Hence the detector is capable of using regions-of-interest (ROI) to select the few stars of relevance and then can perform centroiding to determine the positions of stars within this 1.6'-by-1.6' FoV. Depending on final detector choice and capabilities alongside the final CCS high-pass filter cut-on (currently 40 Hz), the 1 s exposures expected to capture changes in the ELT vibrations of relevance and changes in ELT focal plane distortion will be made up to multiple sub-exposures.

The LGSS is a conventional Shack-Hartmann WFS with design parameters as shown in table 1. As of the date of writing this publication (June 2024) we have not carried out any detailed design work for an optomechanical implementation and assume baseline parameters compatible with existing ELT LGS WFSs (HARMONI).

Table 1. Current LGSS design parameters. We ask the reader to note that we have based this configuration on existing ELT LGS WFS designs and no optimization work has yet been carried out.

<i>Parameter</i>	<i>Value</i>	<i>Comment</i>
sub-aperture sampling	65×65	Not yet optimized
sub-aperture field-of-view	20 arcsec	Preventing excessive spot truncation
sub-aperture pixel sampling	1.3 arcsec	Based on ESO LISA detector
sampling speed	500 Hz	Compatible with PFS
detector RON	$3e^-$	Based on ESO LISA detector

The design of the NGSS as a wide-field imager means that we can select a large number of targets distributed over the FoV of each NGSS, and this is an important design choice which aids the acquisition and guiding functions of GLAO. The first function, acquisition, occurs when the telescope has located a target and the observation has nominally allocated positioners to expected field positions alongside rotation to minimize LGS cutout obscuration by the PFS: MOSAIC can ask the PFS to choose specific guide-stars and so we allocate ours to reduce vignetting. (We will enable this functionality in our sky guiding computation shortly.) In this situation, the NGSS imagers find the positions of known targets and determine the distortion which can reach 117 mas at the edge of our science field. Our requirement is to allocate 99% of positioners to within 40 mas. Once an astrometric solution for the current state of the ELT is obtained, all positioners are shuffled which is a relatively fast process: this two-step positioner control meets the short acquisition requirements.

Once the telescope has begun observing, we then encounter the additional changes in field distortion through relative movements of ELT optics which are only updated sporadically. The edge of our field can move by ≥ 23 mas over an hour. The NGSS therefore continues to provide updates to the instrument (to compensate for rotation) and the telescope (to compensate for X-Y) but we do not move the positioners again after acquisition. This operational design maintains the focal plane displacement on an instrument aperture to between 30 and 57 mas for the field centre on a IFU and field edge on the MOS. A further attractive aspect of the NGSS imager design beyond the ease of selecting any star in the field-of-view is the ability to easily nod and offset the telescope for sky subtraction and calibration: we simply dither the target with software variable changes (no hardware or mechanisms) in the RTC and keep the GLAO loop closed.

3. GLAO SIMULATIONS

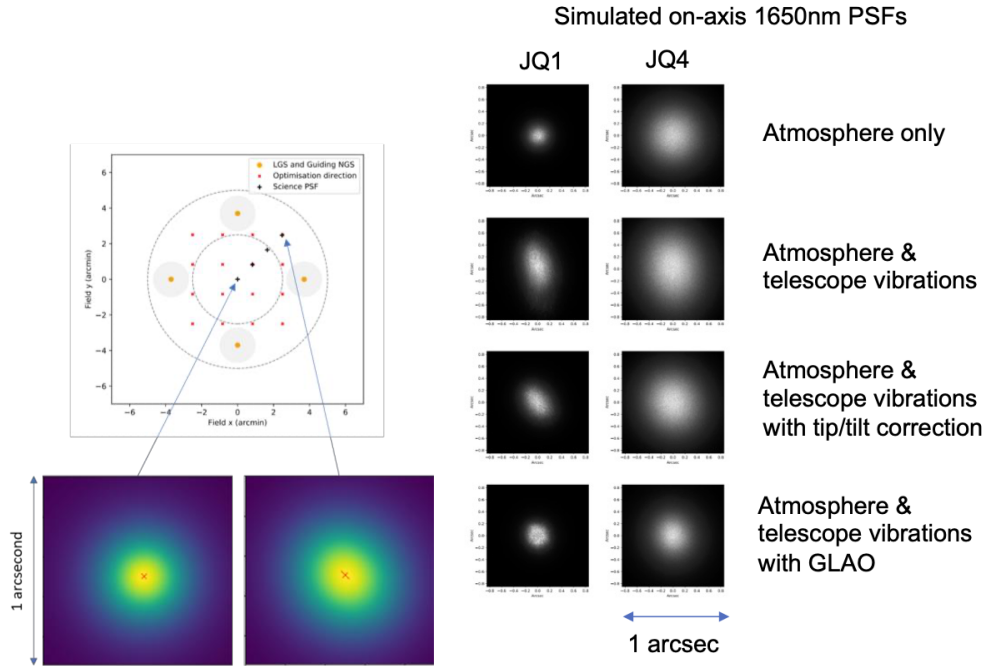


Figure 4. Examples of GLAO simulations for MOSAIC. In all cases, the PSFs are shown in 1 arcsec by 1 arcsec boxes at 1650 nm. (Left) The field dependence of the GLAO PSF is because the ELT M4 mirror is conjugated to +660 m and despite the optimization procedure, the sampling of the wavefront causes a bias towards the centre of the field. (Right) Showing the various aspects we simulate, both inputs (top two rows) and the correction (bottom two rows). The comparison of the top row with the bottom shows that the largest benefit is for the worst seeing (right column, 1.04 arcsec) rather than the best seeing (left column, 0.44 arcsec).

The MOSAIC GLAO design has been supported via simulation to ensure that the requirements are met.

The process involves several steps to move from a AO-only simulation through to including all relevant optical effects which are required to produce an *accurate* PSF to represent the coupling into the fibre interfaces for all spectrographs. The outline of the simulation procedure is:

- Starting with the ANGUS AO simulation code[‡] and using the standard ESO profiles (35-layers) which have variable layer strengths and seeing spanning the interquartiles ranges expected: JQ1 through JQ4, 0.44 arcsec through 1.04 arcsec, and at zenith angle of 45 degrees. ;
 - 4 NGS located in the centre of the LGS cutouts and with no noise simulated ;
 - LGS with no elongation, and tip, tilt, and focus removed via a filtering step ;
 - Introducing a sampled vibration spectrum[§] representing telescope behaviour for all modes specified: tip/tilt through coma inclusive ;
 - Open loop WFS measurements to represent pseudo-open loop control signals: it is simpler since our system does not have to model the ELT CCS and the translation of modal amplitudes into mirror commands and then back again as driven mirror modal amplitudes ;
 - A least-squares reconstructor regularised with the expected C_n^2 statistics via the covariance approach (MMSE) optimized over a 5×5 grid covering the central 2.5' by 2.5' field ;
 - PSFs computed at 0, 70, 140 and 210 arcsec off-axis along a fixed azimuthal angle i.e. along a straight line, and for 10 wavelengths from 400 nm to 1800 nm. ;
- Filtering AO simulation PSFs—in the OTF domain—with static residuals expected from the ELT having amplitudes of 300 nm RMS, to produce Focal Plane PSFs: this allows a set of reference PSFs from the AO simulations to be separated from changes in static aberrations—currently uncertain as regards the *change* over the MOSAIC science field-of-view—as this process is fast (minutes) versus the previous step (hours–days) ;
- Convolution of FP PSFs with rotation and X-Y PDFs from the guiding: currently these uncertainties are assumed normalised distributions with 40 mas in rotation at the edge of the science field and 40 mas in X-Y to represent the limits of our requirements.

A notable omission is the modelling of the interaction between the MOSAIC NGS sensors and the ELT PFS sensors for tip/tilt. At the time of writing, the interface has some outstanding questions therefore we assume, in the simulations, that the PFS measures all tip/tilt signals i.e. without high-pass filtering as specified in the Cascade CCS operating mode. An example of results from the process is shown in figure 4. We do not discuss results in detail here since they are unlikely to be of interest outside the consortium at this stage but we note that the results support our design meeting all requirements.

4. CONCLUSIONS AND FUTURE PROSPECTS

The concept of the ELT MOSAIC instrument has been introduced and the relevant performance requirements for the AO mode—Ground Layer Adaptive Optics—in this instrument has been outlined. As with all ELT instruments, some level of AO is mandatory and whether that is handled by the ELT (via the Pre-Focal Station) or the instrument itself is important for MOSAIC since we choose a hybrid approach—the Central Control System’s Cascade mode which integrates tip/tilt measurements from both the ELT and MOSAIC. For example, the Nasmyth platform movement is expected to reach $\sim \pm 3$ mm which leads to approximately ~ 1 arcsec movement during observations spanning more than a few minutes: the baseline MOSAIC integration is one hour. Therefore it is mandatory from this aspect to have on-instrument guiding. Furthermore the nature of the ELT design leads to focal plane distortions and this must also be measured by the instrument. Therefore the MOSAIC GLAO system is responsible for the pre-observation acquisition measurements to determine the astrometric

[‡]please contact Timothy Butterley, Durham for more details and information on cross-comparisons with P3⁹ and the ESO OCTOPUS simulation for QA.

[§]ESO-271292 2 Telescope Wavefront Perturbations Data Package for the E-ELT Instrument Consortia

solution, and then the during-observation guiding measurements to maintain flux-coupling to the spectrograph apertures. The second key function of the MOSAIC GLAO system is to enhance the flux-coupling by increasing the enclosed energy. Due to the wide field-of-view, the largest of any ELT instrument so far planned, GLAO was the appropriate choice of control mode and this meets the EE increase requirements. Despite being modest, we have produced an innovative and robust design which is validated by simulation results: using four LGS WFS for high-order (beyond focus) measurements, no focus measurement, and tip/tilt measurements via a combination of ELT PFS guide-probes and NGS imager measurements. The lack of mechanisms means that we can easily nod and offset the telescope during an observation since our NGS imagers have large fields-of-view. As a risk mitigation step, for the lack of focus measurement, we reserve the concept of replacing one NGSS imager with a low-order NGS WFS in-order to add focus signal to the AOCM and therefore the ability to control this mode. Our simulations have not indicated that this is required for GLAO correction in itself but instead the addition of focus measurement will permit compensating the defocus at the MOSAIC focal plane from flexures, therefore the NGS WFS would still operate at $\lesssim 80$ Hz.

ACKNOWLEDGMENTS

All authors associated with CfAI, Durham and UKRI-STFC UK ATC acknowledge UKRI funding. In France, MOSAIC has received funding support from the French “ANR-Programme d’Investissements d’Avenir”, referenced as ANR-21-ESRE-0008 and French CSAA/ENG.

REFERENCES

- [1] Pello, R., Puech, M., Prieto, E., Rodrigues, M., Sanchez-Janssen, R., Dalton, G., Ducret, F., Hadi, K. E., García-Vargas, M. L., Lynn, J., Bharmal, N. A., Chapuis, D., Dupieux, M., Hottier, C., Larrieu, M., Martin, L., Mohamed, M., Morris, T., Pérez, A., Seifert, W., Xu, W., Morris, S., Kaper, L., Gallego, J., Afonso, J., Barbuy, B., Contini, T., Finoguenov, A., Kassin, S., Miller, C., Ostlin, G., Pentericci, L., Schaerer, D., Steinmetz, M., Ziegler, B., Araujo, R., Brynnel, J., Castilho, B., Conselice, C. J., Cvetojevic, N., Davison, C., Dejonghe, J., Dessauges-Zavadsky, M., Dohlen, K., Ferreira, D., de Paz, A. G., Gonçalves, T. S., Guinouard, I., Hayes, M. J., Ives, D., Janssen, A., Kehrig, C., Kelz, A., Krajnović, D., Lanotte, A. A., Laporte, N., Laporte, P., Larsen, S., Lemasle, B., Lewis, I., Li, J.-T., Pancino, E., Pieri, M. M., Surace, C., Thurneysen, M., Vergani, S., Wildi, F., Moreno, F. A., Artan, R., Beaulieu, M., Besada, E., Bik, A., Bond, C., Bouri, M., Boy, J., Bramall, D., Brands, S., Braulio, A., Butterley, T., Cabello, C., de Ory, M. C., Calvo, R., Morales, A. C., Challita, Z., Chittik, S., Maldonado, A. C., Frontat, F. D., Dijkstra, E., Elswijk, E., Fasola, G., Feiz, C., Fialho, F., Floriot, J., Franzetti, P., Fumana, M., Gabarra, L., García, L., Gargiulo, A., Gaudemard, J., Giannone, D., Gill, P., Gómez-Gutierrez, A., Gouvret, C., Guenther, A., Harvey, D., nez, J. M. I., Iglesias, J., Ivanisenko, Y., Kunst, P., Kwast, S., Leschinski, K., Licausi, G., Liori, S., Orozco, J. A. L., Lowe, A., Macintosh, M., Magan, H., Maldonado, M., Marquart, T., Martins, L., Melara, M., Melinder, J., Molema, J., Montgomery, D., Morales, M., Najarro, F., Nardetto, N., Navarro, R., Ottomani, A., Pamplona, T., Pannetier, C., Parr-Burman, P., Pascual, S., nataro, M. P., Grande, I. P., Peterzon, J. R., Piqueras, J., Piskunov, N., Cardoso, R. R., Venzal, S. R., Romp, R., Rostami, H., Royer, F., Sablowski, D., Sanchez, A., Blanco, E. S., Schallig, E., Schmoll, J., Schwartz, N., Stephan, J., Taburet, S., Terrett, D., Torralbo, I., Tromp, N., Veredas, G., Yang, Y., and Zeilinger, W., “MOSAIC at the ELT: a unique instrument for the largest ground-based telescope,” in [*Ground-based and Airborne Instrumentation for Astronomy X*], SPIE (2024).
- [2] Chiozzi, G., Kiekebusch, M., Kornweibel, N., Lampater, U., Schilling, M., Sedghi, B., and Sommer, H., “The ELT control system,” in [*Software and Cyberinfrastructure for Astronomy V*], **10707**, 213–229, SPIE (2018).
- [3] Vernet, E., Cerasuolo, M., Cayrel, M., Tamai, R., Kellerer, A., Pettazzi, L., Lilley, P., Zuluaga, P., Diaz Cano, C., Koehler, B., et al., “ELT M4—the largest adaptive mirror ever built,” *The Messenger* **178**(3) (2019).
- [4] Vernet, E., Pirard, J.-F., Hauck, C. A., Ramirez, P. Z., Cayrel, M., Lamour, C., Carel, J. L., Merceron, J. M., Doublet, S., Charuel, C., et al., “ESO ELT M5 unit: design and manufacturing status,” in [*Ground-based and Airborne Telescopes VIII*], **11445**, 729–738, SPIE (2020).

- [5] Lewis, S., Brunetto, E., Förster, A., Frank, C., Guidolin, I., Guisard, S., Hammersley, P., Holzlöhner, R., Jolley, P., Kosmalski, J., et al., “Extremely large telescope prefocal station A system concept,” in [*Ground-based and Airborne Telescopes VII*], **10700**, 407–425, SPIE (2018).
- [6] Morris, T., Basden, A., Calcines-Rosario, A., Dohlen, K., Dubbeldam, C., El Hadi, K., Fitzsimons, E., Fusco, T., Gendron, E., Hammer, F., et al., “Phase A AO system design and performance for MOSAIC at the ELT,” in [*Adaptive Optics Systems VI*], **10703**, 374–386, SPIE (2018).
- [7] La Penna, P., Förster, A., Frank, C., Guidolin, I., Guisard, S., Hammersley, P., Holzlohner, R., Jolley, P., Kosmalski, J., Lampater, U., et al., “ELT Pre-Focal Station NGS Sensor Arm,” *Proc. AO4ELT5* (2017).
- [8] Nijenhuis, J. R., Jonker, W., and Kamphues, F., “Development of a laser projection system for the ELT,” in [*Astronomical Telescopes + Instrumentation*], (2022).
- [9] Neichel, B., Beltramo-Martin, O., Plantet, C., Rossi, F., Agapito, G., Fusco, T., Carolo, E., Carlà, G., Cirauolo, M., and Van Der Burg, R., “TIPTOP: a new tool to efficiently predict your favorite AO PSF,” in [*Adaptive Optics Systems VII*], **11448**, 603–614, SPIE (2021).
- [10] Marchetti, E., Amico, P., Brinkmann, M., Conzelmann, R. D., del Valle, D., di Lieto, N., Engelhardt, M., Geimer, C., Hopgood, J., Molina, I., Mueller, E., Quentin, J., Reyes, J., Richerzhagen, M., Seidel, M., Stegmeier, J., and Todorovic, M., “Final performance of the ESO’s ALICE and LISA wavefront sensing cameras,” in [*Astronomical Telescopes + Instrumentation*], (2022).